Functional Properties of Human Hemoglobins Synthesized from Recombinant Mutant β-Globins†

Michael L. Doyle,‡ George Lew,‡ Alice De Young,§ Laura Kwiatkowski,§ Anita Wierzba,§ Robert W. Noble,§ and Gary K. Ackers*,‡

Department of Biochemistry and Molecular Biophysics, School of Medicine, Washington University, St. Louis, Missouri 63110, and Departments of Medicine and Biochemistry, School of Medicine, Veterans Administration Medical Center, State University of New York at Buffalo, New York 14215

Received February 7, 1992; Revised Manuscript Received June 12, 1992

ABSTRACT: The previous and following articles in this issue describe the recombinant synthesis of three mutant β-globins (β1 Val → Ala, β1 Val → Met, and the addition mutation β1 + Met), their assembly with heme and natural α chains into $\alpha_2\beta_2$ tetramers, and their X-ray crystallographic structures. Here we have measured the equilibrium and kinetic allosteric properties of these hemoglobins. Our objective has been to evaluate their utility as surrogates of normal hemoglobin from which further mutants can be made for structure–function studies. The thermodynamic linkages between cooperative oxygenation and dimer–tetramer assembly were determined from global regression analysis of multiple oxygenation isotherms measured over a range of hemoglobin concentration. Oxygen binding to the tetramers was found to be highly cooperative (maximum Hill slopes from 3.1 to 3.2), and similar patterns of O_2-linked subunit assembly free energies indicated a common mode of cooperative switching at the $\alpha^1\beta^2$ interface. The dimers were found to exhibit the same noncooperative O_2 equilibrium binding properties as normal hemoglobin. The most obvious difference in oxygen equilibria between the mutant recombinant and normal hemoglobins was a slightly lowered O_2 affinity. The kinetics of CO binding and O_2 dissociation were measured by stopped-flow and flash photolysis techniques. Parallel studies were carried out with the mutant and normal hemoglobins in the presence and absence of organic phosphates to assess their allosteric response to phosphates. In the absence of organic phosphates, the CO-binding and O_2 dissociation kinetic properties of the muant dimers and tetramers were found to be nearly identical to those of normal hemoglobin. However, the effects of organic phosphates on CO-binding kinetic properties of the mutants were not uniform: the β1 + Met mutant was found to deviate somewhat from normalcy, while the β1 Val → Met mutant reproduced the native allosteric response. Further characterization of the allosteric properties of the β1 Val → Met mutant was made by measuring the pH dependence of its overall oxygen affinity by tonometry. Regulation of oxygen affinity by protons was found to be nearly identical to normal hemoglobin from pH 5.8 to 9.3 (0.52 ± 0.07 protons released per oxygen bound at pH 7.4). The present study demonstrates that the equilibrium and kinetic functional properties of the recombinant β1 Val → Met mutant mimic reasonably well those of normal hemoglobin. We conclude that this mutant is well-suited to serve as a surrogate system of normal hemoglobin in the production of mutants for structure–function studies.

With the successful expression of human β-globin in *Escherichia coli*, and its isolation and assembly into the tetrameric $\alpha_2\beta_2$ hemoglobin (Hernan et al., 1992), we consider here the functional consequences arising from the amino terminal processing specificity of *E. coli*. In humans the β-globin gene codes for the amino terminal sequence Met-Val-His···. The terminal Met is then removed by processing enzymes to yield the authentic sequence Val-His···. However, the enzyme processing system of *E. coli* has a different specificity for amino terminal processing which does not remove the Met residue. Thus, it has not been possible to produce authentic human β-globin directly from *E. coli*.

The first reports of recombinantly produced human β-globin involved expression of β-globin as a fusion protein (Nagai & Thøgersen, 1984; Nagai et al., 1985). The authentic β-globin was then purified following an in vitro enzymatic cleavage step. More recently, "mutant" α- and β-globins were expressed directly from *E. coli* without further enzymatic processing (Hoffman et al., 1990). Despite the existence of an extra amino terminal methionine on these α and β chains, the functional properties of the resulting hemoglobin were quite similar to those of normal Hb. Each of these hemoglobin syntheses, and a recent report of the use of yeast as an expression system (Wagenbach et al., 1991), have demonstrated the ability of recombinant methods to produce human Hb with high cooperativity and reasonable allosteric response to pH and organic phosphates.

Our strategy for synthesizing recombinant human Hb for use in structure–function studies begins with the production of three particular mutant β-globins from *E. coli*, reasoning that one or more will mimic normal β-globin precisely enough to serve as a surrogate system from which further mutants can be produced. The mutants of interest involve substitution of β1 valine by amino acids with uncharged side chains of moderate size. We expect that these modifications will be nearly inconsequential to function, based on the molecular location of the residue (external), and the likelihood that any allosteric role for β1 Val would probably originate from interactions with the more reactive amino group, rather than the isopropyl side chain.

† This work was supported by NIH Grants HL 40453 and GM 24486, NSF Grants, 91-07244 and DMB 9107244, and research funds from the Veterans Administration.

* Address correspondence to this author.
‡ Washington University.
§ State University of New York at Buffalo.

0006-2960/92/0431-8629$03.00/0

The three mutants that we have synthesized are the following: (1) β1 + Met, the "default" addition mutation generated from the authentic β-globin gene, as described above; (2) β1 Val → Met, obtained by deleting the nucleotide triplet that codes for β1 Val; and (3) β1 Val → Ala, obtained by modifying the β1 codon so as to code for alanine instead of valine. Since the amino terminal processing system of *E. coli* effectively removes amino terminal methionines that are adjacent to alanine, the resulting amino terminal residue is alanine. Purification of these β-globins, refolding with the heme prosthetic group, and assembly with natural human α chains to form $\alpha_2\beta_2$ tetramers is described by Hernan et al. (1992).

The objective of the present study is to evaluate the allosteric functional properties of these recombinant β-chain synthetic Hbs. The functional properties examined include (1) the kinetics of CO binding to the deoxygenated Hb's, as measured by rapid mixing of the reactants and also by flash photolysis of the carbonmonoxyHb's; (2) the kinetics of O_2 dissociation; (3) the allosteric effects of organic phosphates and pH on CO-binding kinetics and oxygenation equilibria by tonometry, respectively; and (4) the thermodynamic linkage between dimer–tetramer assembly and cooperative oxygenation (Ackers & Halvorson, 1974) as described by eq 1. The latter data provide a measure of the homotropic cooperative interactions between heme sites within tetramers and dimers. Moreover, evaluation of dimer–tetramer assembly free energies at intermediate oxygenation states provides a sensitive measure of cooperativity-linked structure changes at the critical $\alpha^1\beta^2$ interface. At the same time, the kinetic measurements offer a comparison of the CO-binding kinetic properties of both tetramers and dimers, independent estimation of dimer–tetramer assembly free energies, and a rapid means for exploring the allosteric effects of organic phosphates and pH.

EXPERIMENTAL PROCEDURES

Materials. Native human Hb[1] was obtained from hemolysates of freshly drawn blood as described by Geraci et al. (1969). After lysis, NaCl was added to a concentration of 0.1 M followed by centrifugation at 40000*g*. Following careful separation from the cell debris, the supernatant was passed through a Sephadex G-25 coarse column equilibrated with 1 mM Tris, pH 8.4. The eluate was passed through a Dintzis column of mixed-bed resins to remove organic phosphate (Riggs, 1981). For purposes of kinetic comparison of mutant and normal human Hbs, this stripped hemolysate is kinetically indistinguishable from HbA_0, due to the similarities in the ligand-binding kinetics of the minor components and their low abundances (Steinmeier & Parkhurst, 1975). We note that the subunit assembly and oxygen equilibrium parameters for HbA_0 referred to in the present study were taken from Chu et al. (1984), where the minor Hb components were removed by anion exchange.

The mutant hemoglobins, β1 Val → Ala, β1 Val → Met, and β1 + Met, were obtained by molecular biological techniques described by Hernan et al. (1992). These hemoglobins were assembled and purified in the presence of CO to enhance their stability, particularly against autoxidation of heme iron. Prior to the equilibrium measurements and stopped-flow kinetic measurements, the CO derivatives were photodissociated with a fluorescent light while being flushed with an atmosphere of humidified oxygen. The sample was kept on ice during this procedure. Visible spectra were periodically measured until a fully oxygenated spectrum was obtained. Absorbance changes upon addition of potassium cyanide to these materials and the ratio of absorbances 576 nm/560 nm and 540 nm/560 nm indicated only very small amounts of methemoglobin or residual CO derivative. For some experiments, the CO-bound mutants were also passed through a Dintzis column to remove ions.

Stock solutions (100 mM) of DPG were prepared from the diTris salt (Sigma) without pH adjustment; 200 mM stock solutions of IHP were prepared from the sodium salt (Sigma). The pH of the IHP solution was adjusted to 5.6 by titration with the acid form of Amberlite IR-120 resin, which allowed final pH adjustment without the addition of anions such as chloride to the samples.

Deoxygenated Subunit Assembly Equilibrium by Haptoglobin Kinetics. The equilibrium between deoxygenated dimers and tetramers was determined from forward and reverse reaction rate constants. The dissociation rate constant was measured by the haptoglobin technique as described previously (Ip et al., 1976). Time courses were monitored spectrophotometrically in the Soret region with a Cary 219 spectrophotometer. The equilibrium constant for the deoxygenated subunit assembly reaction, ${}^0K_2$, was calculated from the measured dissociation rate constant and an association rate constant of 1.1 (±0.2) × 10^6 M^{-1} s^{-1}, a consensus value which is invariant over a wide range of pH, temperature, and mutagenic perturbation (Turner, 1989).

Oxygenation Isotherms. Oxygen-binding isotherms were measured with a continuous-flow spectrophotometric method (Imai, 1978) as described previously (Chu et al., 1984). All oxygenation and haptoglobin kinetic measurements were performed in 0.1 M Tris, 0.1 M NaCl, and 1 mM Na_2EDTA, 21.50 °C, and pH 7.40 (0.18 M chloride total). The Hb sample in the cell was equilibrated against 1 atm humidified oxygen. Deoxygenation was carried out by flushing the stirred sample with humidified nitrogen gas (O_2-free grade, Linde Gases). The oxygen fractional saturation was monitored with a Cary 4 spectrophotometer at 415 nm for concentrations of 5.77 μM heme or less, 600 nm for concentrations of 80 μM or more, and 415 nm for the remaining data. Oxygen activity was measured with a Beckman 39065 O_2 probe. Temperature in the sample cell was regulated within ± 0.02 °C by means of a Model PTC-36 Tronac precision temperature controller (Tronac, Inc., Orem, UT). The precision and accuracy of the temperature in the sample cell was measured with a National Bureau of Standards calibrated thermistor probe/Cole-Parmer 8502-20 digital thermometer. The pO_2 data were collected in equal increments of time (1–2 s per observation) as voltage measurements from the oxygen electrode system with a Nicolet Model 3091 digital oscilloscope and absorbance data recorded directly with the Cary 4. Typical deoxygenation time was 30–45 min. The data were plotted on 8 × 11 in. paper as absorbance versus logarithm molarity O_2 and digitized with a Hewlett-Packard 9111a graphics tablet in equal increments of the logarithm of the O_2 activity. Reversibility was tested by comparing deoxygenation and reoxygenation absorbance traces and showed return to the initial absorbance to within 2–3% of the total absorbance change. Oxidation of the hemoglobins was minimized by the addition of an enzymic reducing (Hayashi et al., 1973) just prior to measuring each isotherm. Typical accumulation of methemoglobin during

[1] Abbreviations: Bis-tris, bis(2-hydroxyethyl)iminotris(hydroxymethyl)methane; DPG, 2,3-diphospho-D-glyceric acid; HbA_0, human hemoglobin major component; HbA, human hemoglobin hemolysate stripped of organic phosphates; IHP, inositol hexaphosphate; metHb, hemoglobin with iron oxidized to Fe(III); Na_2EDTA, disodium ethylenediaminetetraacetate; Tris, tris(hydroxymethyl)aminomethane.

the deoxygenation–reoxygenation process was estimated to be 1–3%.

Data Analysis for Subunit Assembly and Oxygenation Data. The linkage between oxygenation of the Hb system and dimer–tetramer assembly is outlined in eq 1.

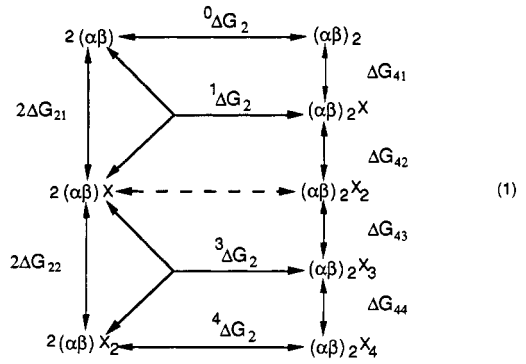

(1)

Free energy changes are adjacent to arrows which represent equilibria (see Appendix for definitions). The dashed arrow at the doubly ligated tetrameric state indicates that there are two ligand stoichiometry combinations of dimers which contribute to its formation.

Global regression analysis of oxygenation isotherms collected over a range of hemoglobin concentration was based on eq 2, where $A(X_i)$ is the ith observed absorbance value at

$$A(X_i) = A_0 + (A_\infty - A_0)\bar{Y}(X_i) \qquad (2)$$

O_2 activity X_i, $\bar{Y}(X_i)$ is the fractional saturation (Appendix, eq A1) at X_i, and A_0 and A_∞ are the asymptotic absorbance values for zero and infinite O_2 activities, respectively. Since eq 2 assumes the observed absorbancies are directly proportional to fractional saturation, critical assessment of the Soret and visible isosbestic conditions for the $\beta 1$ recombinant mutant hemoglobins at intermediate saturations was carried out. The results indicated reasonable validity of this assumption, being very similar to the reported isosbestic behavior of normal human hemoglobin (Doyle et al., 1988).

The functional form of the fitting equation for $\bar{Y}$ (eq A1) contained the Gibbs free energies corresponding to the equilibrium constants K_{41}, K_{42}, K_{43}, K_{44}, $^4K_2$, and k_{22}. This choice of parameters originates from the fact that the deoxy $\alpha\beta$ dimer does not exist to any appreciable degree at the "high" Hb concentrations studied (i.e., above nanomolar) when the deoxy dimer–tetramer assembly free energy is very favorable (as is the case for all Hbs in the present study). All other species in eq 1 can be shown to make substantial contributions to the experimental data of the present study. While the deoxy dimer species was not included in the partition function, equilibria involving the deoxy dimer ($^0K_2$ and k_{21}) were determined from the resolved fitting parameters above and the independently measured value of $^0K_2$ by conservation of energy. After regression analysis, the data were converted to $\bar{Y}$ values for illustrative purposes.

Nonlinear least-squares analysis was carried out with the program NONLIN (Johnson & Frasier, 1985). The program employs a modified Gauss–Newton algorithm to find the most probable values of the adjustable parameters and evaluates upper and lower confidence limits by searching variance space for an F-statistic corresponding to 67% confidence probability (Ackers et al., 1975; Johnson et al., 1976). Standard errors for those parameters which were not directly fitted for were propagated [cf. Bevington (1969)]. All data points were weighted equally on a fractional saturation basis for reasons described previously (Doyle & Ackers, 1992). Median ligand activities (Appendix, eq A5) were measured by planimetry from data plotted on 8 × 11 in. paper as absorbance versus logarithm oxygen activity.

Kinetics of CO Binding by Flash Photolysis. Kinetics of CO recombination following complete photodissociation of the ligand were measured with an apparatus consisting of an optical system and three photographic strobe units (Sunpak Auto 544) equipped with thyristor quenching devices. Data were collected and processed by an On-line Instrument Systems (OLIS) Model 4000 data aquisition and control system (Jefferson, GA). The strobes were adjusted to give a rectangular light pulse, approximately 0.5 mS in duration. To ensure no contribution of the flash to the observed rate process, data collection was delayed 1.2 mS after initiation of the flash. The progress of the reaction was monitored at 420 and 435 nm. To further reduce interference between the flash and monitoring of light transmission, the flash radiation was filtered through a solution of auramine, which has high extinction coefficients at the monitoring wavelengths. The concentration of heme was usually 5 μM, while CO was at least 10-fold higher to permit the use of the first-order rate equation as an approximation to the time course of the reaction. An anaerobic water-jacketed cylindrical cuvette with a path length of 1.0 cm was used, and a small amount of dithionite (<50 μM) was added to remove residual oxygen.

Kinetics of CO Binding and O_2 Dissociation by Stopped Flow. The rate of CO combination with deoxygenated Hb was measured in a stopped-flow apparatus similar to that described by Gibson and Milnes (1964). The procedures used were essentially those first described by Gibson (1959). Reactions were followed in a 2.0-cm cell at 420 and 435 nm at 20 °C. The final heme and CO concentrations were generally 2.5 and 25–50 μM, respectively. Dithionite concentrations of 2.0 mM were used to maintain anaerobicity. An on-line computer with OLIS instrumentation and software was used for data aquisition and manipulation.

The overall rate of oxygen dissociation from Hb was measured by stopped flow at 20 °C by rapid mixing of oxyHb with a solution of dithionite. A 2-mm cell was used to allow the use of higher concentrations of Hb (15 μM heme). This significantly diminished the rate of metHb formation in the oxyHb solutions. To eliminate contributions of ferric to ferrous heme upon exposure to the dithionite, an isosbestic point was determined for deoxy- and methemoglobin and the oxygen dissociation followed at the isosbestic point.

All kinetic measurements were carried out so as to allow precise comparison between HbA and the mutant Hb's. Thus, comparison of the HbA and mutant rates for a particular pH and organic phosphate concentration was performed on the same day using the same buffer and total ligand concentration. The relative precision of the rates determined in this manner is a few percent, whereas the reproducibility of multiple determinations is approximately 10%.

All ligand-binding kinetic data were fitted to one or two exponentials. A method based on multiple integrations was used (Matheson, 1987). The resulting fits provided rates, amplitudes, and standard errors for the fitting parameters. The quality of the fits were judged visually and also with a Durbin–Watson test of the variance of the residuals [cf. Draper and Smith (1981)].

Oxygen Equilibria by Tonometry. Some oxygen-binding curves were measured by tonometry essentially by the Nagel et al. (1965) modification of the method of Allen et al. (1950). A 500-mL tonometer with an attached 1-cm cuvette was used. The Hb concentration was 50 μM heme. Spectral measure-

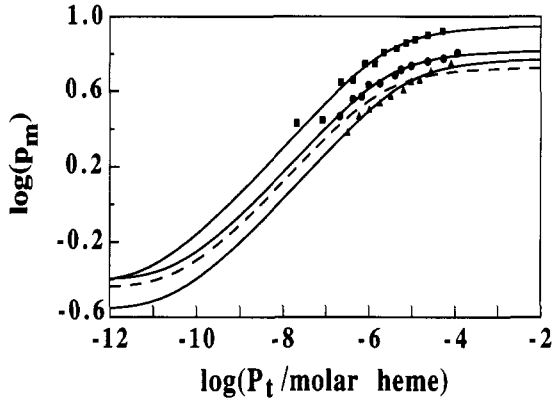

FIGURE 1: Logarithm of median O_2 partial pressures, p_m (Torr), for oxygenation of recombinant mutant Hb's as a function of the logarithm of the Hb concentration, P_t (heme units). Data are for mutants β1 Val → Met (■), β1 Val → Ala (●), and β1 + Met (▲). The curves represent best fits for regression analysis to eq A5. The dashed curve corresponds to normal Hb (Chu et al., 1984). Solution conditions: 0.1 M Tris, 0.1 M NaCl, and 1 mM Na_2EDTA, 21.50 °C, and pH 7.40 (0.18 M chloride total).

ments were carried out with a Cary 14 spectrophotometer modified by OLIS for computer control and on-line data aquisition.

Buffers used in the tonometry, flash photolysis, and stopped-flow experiments were prepared by titrating HCl against the base form of either bis-Tris (pH 5.8–7.2) or Tris (pH 7.2–9.3) and then diluting the resulting solution with deionized water to a final chloride concentration of 0.1 M. Thus, while there were differences in concentration of buffer, the stronger allosteric effector, chloride (Haire & Hedlund, 1977; Imaizumi et al., 1979), was constant for all pH's. Deoxygenation was accomplished by equilibration with oxygen-free nitrogen.

RESULTS

Overall Energetics: Oxy and Deoxy Subunit Assembly and Average Oxygen Affinities of Dimers and Tetramers. The median partial pressure,[2] p_m, for an oxygenation isotherm of human hemoglobin is a function of Hb concentration, due to the equilibrium between dimers and tetramers (Mills et al., 1976; Chu et al., 1984). Thus, the observed p_m at a given Hb concentration reflects the oxygen-binding properties of both dimers and tetramers. The dependence of p_m on Hb concentration is described exactly by eq A5 in terms of the oxy and deoxy dimer–tetramer assembly equilibria ($^4K_2$ and $^0K_2$, respectively) and the overall equilibrium constant for binding four oxygens to the tetramer form (K_{44}). This functional dependence can be exploited for an experimental determination of these parameters by measuring p_m versus Hb concentration. Figure 1 shows the median oxygen partial pressures for each of the three recombinant hemoglobins measured over a range of hemoglobin concentrations. According to eq A5, the parameter K_{44} is determined essentially equally well at any Hb concentration, while the parameters $^4K_2$ and $^0K_2$ are determined most precisely by the curvatures approaching the upper and lower asymptotes, respectively. Since the lower limit of Hb concentration that can be studied is approximately 100 nM heme, $^0K_2$ was determined independently by haptoglobin kinetics procedures (see Experimental Procedures) and constrained during regression analysis. The results for fitting the median data in Figure 1 to eq A5 are given in Table I as free energies. The equilibrium constant for binding two

[2] The median ligand activity is used in this instance rather than the p_{50} by virtue of its exact thermodynamic identity (see Appendix).

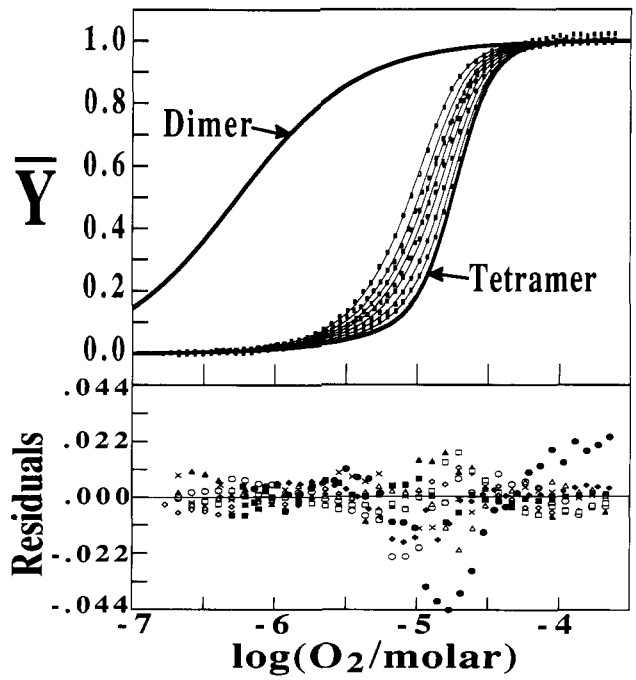

FIGURE 2: (Top) Oxygenation isotherms of the recombinant mutant hemoglobin β1 Val → Met at different Hb concentrations (0.426, 0.819, 1.39, 2.25, 4.48, 7.42, 12.1, 23.7, and 52.2 μM in heme units). Every other data point is shown as an x. The smooth curves superposed with the data represent the best least-squares fit to eq 2. The predicted curves for O_2 binding to pure dimers and tetramers are shown on the far left and right, respectively. Conditions are given with Figure 1. (Bottom) Residuals ($\bar{Y}$ units) for the simultaneous fit of nine isotherms to eq 2. Every fifth residual is plotted. Heme concentrations: 52.2 (△), 23.7 (◇), 12.1 (□), 7.42 (○), 4.48 (▲), 2.25 (◆), 1.39 (■), 0.819 (●), and 0.426 μM (×). Square root of the variance for the global fit of eight isotherms was 0.00818 in $\bar{Y}$ units with 1474 degrees of freedom.

oxygens to Hb dimers, K_{22}, was then determined by conservation of energy from the values of $^4K_2$, $^0K_2$, and K_{44} (see eq 1).

Subunit Assembly and Intermediate Oxygenated States. Equilibria involving the intermediate ligation states (eq 1) were determined by simultaneous fitting of isotherms measured over a range of Hb concentrations (eqs 2 and A1). Figure 2 shows a representative set of oxygenation isotherms for the β1 Val → Met mutant measured over a range of hemoglobin concentrations. The best-fit parameters from the fit are summarized for all three recombinant Hbs in Figure 3. Typically 10–12 isotherms were measured over a range of Hb concentrations, and 1–2 of these isotherms were regarded as outliers based on examination of residuals for the global fit. Close examination of the residuals for individual isotherms indicates small systematic deviations. These systematic trends are likely to originate mostly from formation of methemoglobin (typically 1–3%), which is of particular concern at intermediate oxygenation states. Due to the poor resolvability of the individual parameters ΔG_{42} and ΔG_{43}, we report the sum of these two intrinsic free energies, which is determined robustly. The low resolvability of intermediate-state free energies is typical for highly cooperative systems (where the populations of the intermediates are low) and is exacerbated by the presence of small systematic errors, such as metHb formation.

It should be noted that the two oxygen-binding steps of the dimer are determined by two measurements: the last step by global regression analysis of multiple isotherms and the first step by conservation of energy (eq 1) together with the independently measured value of the deoxy dimer–tetramer assembly equilibrium constant, $^0K_2$ (see Experimental Pro-

Table I: Overall Subunit Assembly and Oxygenation Free Energies for Normal Hb and Recombinant Mutant Hbs Determined by Analysis of Median Partial Pressures[a]

system	$^4\Delta G_2$/kcal	ΔG_4/kcal	$^0\Delta G_2$[b]/kcal	ΔG_2[c]/kcal
normal HbA_0[d]	−8.05 ± 0.1	−27.09 ± 0.05	−14.35 ± 0.1	−16.69 ± 0.20
β1 Val → Ala	−7.84 ± 0.12	−26.61 ± 0.07	−14.4 ± 0.1	−16.59 ± 0.17
β1 Val → Met	−7.84 ● 0.29	−25.89 ± 0.18	−15.2 ± 0.1	−16.63 ± 0.36
β1 + Met	−7.31 ● 0.12	−26.84 ± 0.12	−14.5 ± 0.1	−17.02 ± 0.20

[a] Conditions: 0.1 M Tris, 0.1 M NaCl, and 1 mM Na_2EDTA, 21.50 °C, and pH 7.40 (0.18 M chloride total). [b] Determined by haptoglobin kinetics [c] Calculated by conservation of energy from the other parameters. [d] Values from Chu et al. (1984).

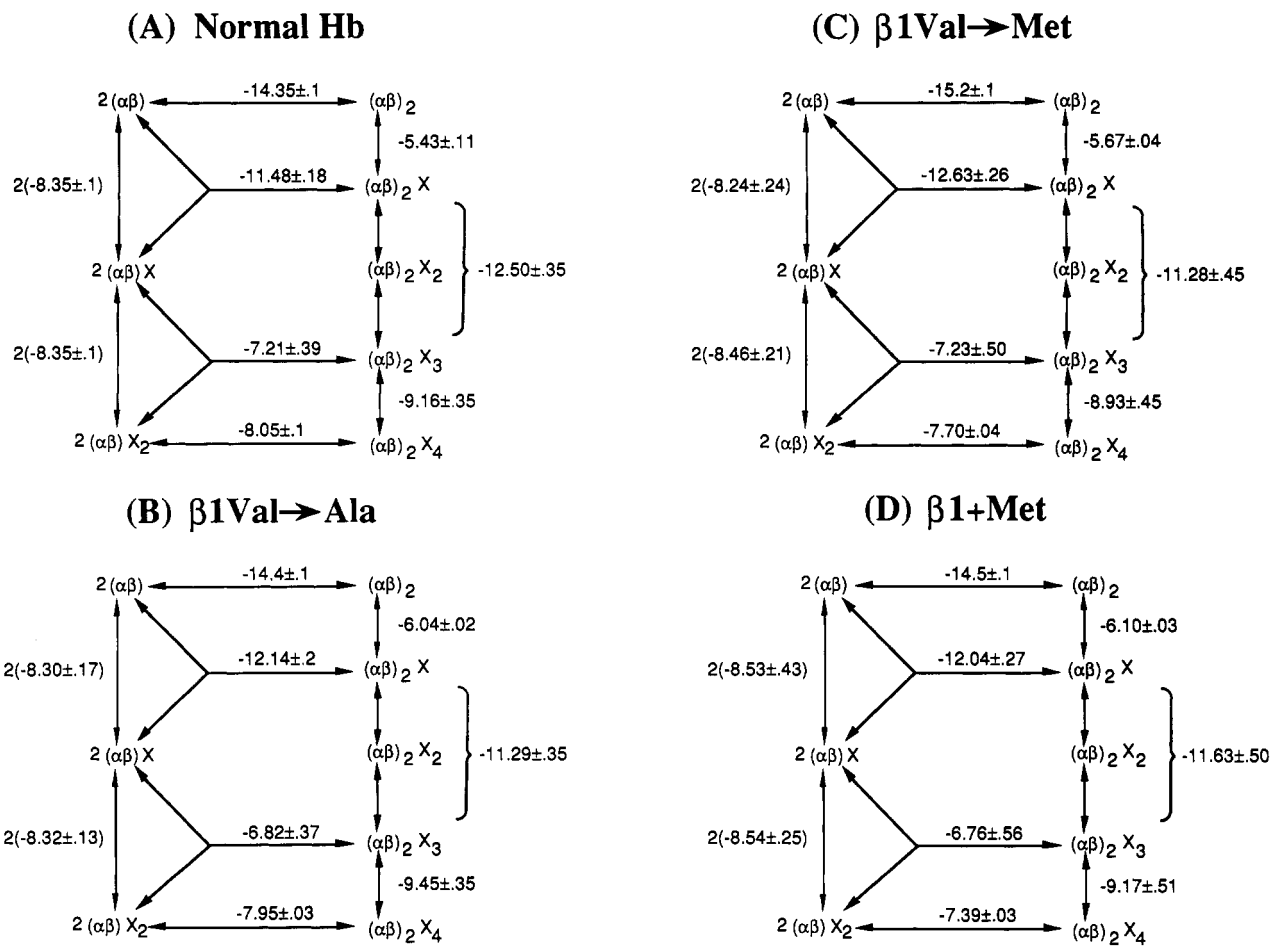

FIGURE 3: Thermodynamic linkage parameters for O_2-linked dimer–tetramer assembly of (A) normal Hb and the recombinant mutant Hb's (B) β1 Val → Ala, (C) β1 Val → Met, (D) β1 + Met. Parameters were determined by global regression analysis of multiple isotherms. Hb concentrations studied: (A) see Chu et al. (1984); (B) 0.417, 0.666, 1.83, 4.14, 5.77, 9.99, 24.0, and 59.0 μM heme; (C) see Figure 2 legend; and (D) 0.313, 0.575, 1.01, 1.78, 3.17, 6.51, 9.97, 15.7, 28.4, and 82.7 μM heme. Intrinsic free energies (corrected for statistical degeneracies) are in kilocalories. The intrinsic free energies of the second and third steps are shown as their sum due to poor resovability of the individual steps. The largest deviation of the upper and lower 67% confidence limits is shown as the standard error on each parameter. The square root of the variance (in $\bar{Y}$ units) for each of the global fits was 0.00412, 0.00447, 0.00818, and 0.00859 for A–D, respectively.

cedures for further details). The self-consistency of the observed noncooperativity determined for the dimers of all three β1 mutants and normal Hb attests to the degree of accuracy of the experimental methods used.

Kinetics of CO Binding and Allosteric Responses of Organic Phosphates and pH. Carbon monoxide binding kinetics were measured by stopped flow, whereby deoxygenated Hb is mixed with CO and the combination reaction is followed spectrophotometrically, and also by flash photolysis, whereby the CO-saturated molecules are fully photolyzed to the deoxygenated state by a pulse of light and the recombination reaction is monitored spectrophotometrically. The two techniques differ fundamentally: in the former case the initial state of Hb is deoxy, where the system exists virtually as tetramers, and in the latter technique the initial state of the Hb is CO-saturated, where the system consists of dimers and tetramers. Therefore, in the stopped-flow experiment one observes kinetic properties of the tetramer, while in the flash photolysis experiments two kinetic phases are expected, a rapid phase due primarily to $\alpha\beta$ dimers and a slow phase representing CO recombination with $\alpha_2\beta_2$ tetramers. For cases where the overall ligand affinity of tetramers differs from that of dimers, the combination of these two techniques permits evaluation of the ligand-binding kinetic properties of both tetramers and dimers. Moreover, the relative amplitudes of the two phases in the flash photolysis experiments afford an independent estimate of the tetramer–dimer assembly free energy.

Figure 4 shows the time courses of CO recombination with normal Hb and the mutant Hb's following flash photolysis. The fast and slow phases seen for each hemoglobin differ in rate by roughly 30-fold. Providing that the two phases originate from dimers (fast) and tetramers (slow) and that

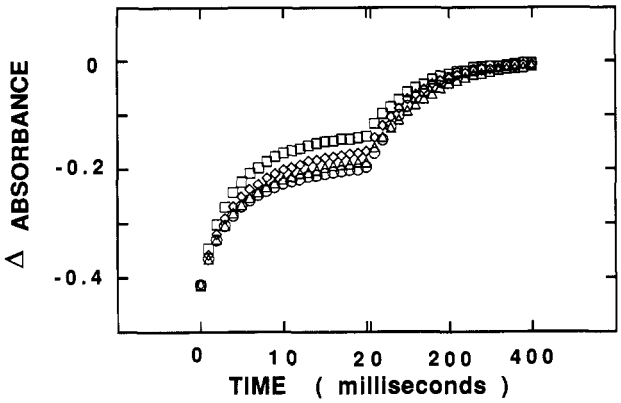

FIGURE 4: Time course of recombination of CO with HbA (○), β1 Val → Met (△), β1 Val → Ala (◇), and β1 + Met (□) following flash photolysis. The change in absorbance at 420 nm is plotted as a function of time. In order to visualize the two kinetic phases the time axis is discontinuous. It is linear from 0 to 20 ms at which point the scale is enlarged by a factor of 20 and is again linear from 20 to 400 ms. The double line at 20 ms indicates the change in scale. Measurements were carried out at 20 °C in bis-Tris, 100 mM chloride, pH 7.0, 4.8 μM in heme, and 48 μM CO.

Table II: Comparison of Dimer–Tetramer Assembly Free Energies, $^4\Delta G_2$, Measured by Flash Photolysis and Concentration Dependence of Oxygenation Isotherms[a]

hemoglobin	flash photolysis[b]	oxygenation isotherms[c]
HbA	−7.8 ± .2	−8.05 ± .10[d]
β1 Val → Ala	−7.6 ± .2	−7.95 ± .03
β1 Val → Met	−7.7 ± .2	−7.70 ± .04
β1 + Met	−7.2 ± .2	−7.39 ± .03

[a] All values are in kilocalories. [b] Conditions: bis-Tris and 100 mM chloride, pH 7, and 20 °C. [c] Conditions: 0.1 M Tris, 0.1 M NaCl, and 1 mM Na_2EDTA, 21.50 °C, and pH 7.40 (0.18 M chloride total). [d] Determined directly by analytical gel chromatography (Ackers, 1970; Chu et al., 1984).

the dimer–tetramer association rate is much slower [see Doyle et al. (1991)], then the ratio of the two amplitudes allows an estimate of the equilibrium constant for dimer–tetramer assembly under fully liganded conditions. The assembly free energies predicted by this procedure (Table II)[3] are found to agree well with those obtained by global analysis of oxygenation isotherms (above).

The effect of IHP on the relative amplitudes of the flash photolysis kinetic phases provides a rapid means for evaluating the allosteric response of the dimer–tetramer equilibrium to organic phosphates. The results of such an analysis are summarized in Figure 5, where it can be seen that at lower concentrations of IHP tetramer formation is enhanced whereas at higher concentrations of IHP dissociation into dimers occurs. A minimum proportion of fast phase (presumably where the lowest proportion of dimers exists) is observed at 0.1–0.2 mM IHP, in very good agreement with previous work, which found a maximum stability of the tetramer in this concentration range (Hensley et al., 1975; White, 1976). The data for the β1 Val → Met mutant reproduce the behavior of normal Hb most precisely, whereas the β1 Val → Ala mutant is the most dissimilar to normal Hb, indicative of greater IHP-induced dissociation into dimers. The second-order rate constants for the two kinetic phases for each Hb in the absence of organic phosphates are reported in Table III. The fast phases all

[3] The pH difference between the two sets of experiments corresponds to a first-order correction of an additional −0.3 kcal in going from pH 7 to pH 7.4 (Chu & Ackers, 1981; Turner, 1989). The small temperature difference is insignificant (Mills & Ackers, 1979a).

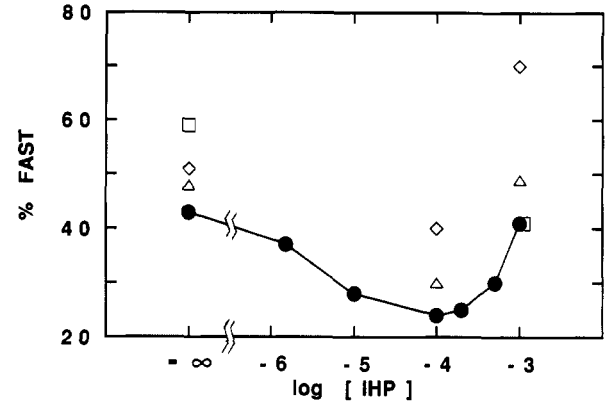

FIGURE 5: Effect of IHP on the relative contribution of the fast phase for CO recombination with HbA (●), β1 Val → Met (△), β1 Val → Ala (◇), and β1 + Met (□). The percent fast phase, an estimate of the percentage of αβ dimers relative to $(\alpha\beta)_2$ tetramers, is plotted versus the logarithm of IHP concentration. Measurements were carried out at 20 °C in bis-Tris, 100 mM chloride, pH 7.0, 4.8 μM in heme, and 48 μM CO.

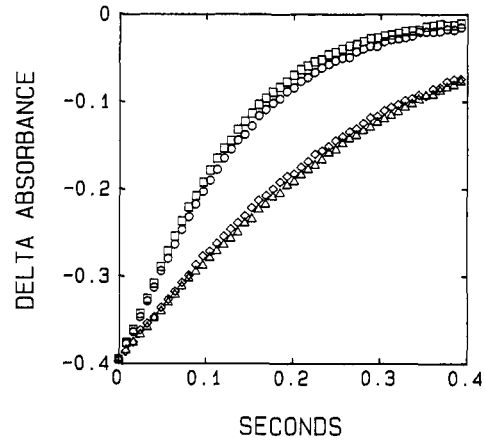

FIGURE 6: Comparison of effects of 1 mM IHP on the time course of CO combination with deoxygenated HbA and the mutant β1 Val → Met as measured by stopped-flow methods. The absorbance change at 420 nm is plotted as a function of time. Data shown are for HbA in the absence (□) and presence (△) of IHP and for the recombinant mutant in the absence (○) and presence (◇) of IHP. Measurements were carried out at 20 °C in bis-Tris, 100 mM chloride, pH 7.0, 2.3 μM in heme, and 48 μM CO.

exhibit similar rates and are those normally attributable to the αβ dimers. The slow phases are also quite similar, although the tetrameric rates are most precisely determined by stopped-flow measurements because dimers are essentially absent.

The combination of CO with the deoxygenated Hb's was measured by stopped-flow methods in the absence and presence of organic phosphate. All experiments were thus carried out in sets of four, allowing examination of the effect of organic phosphate and comparison to normal Hb under identical conditions. Representative time courses for these reactions are shown in Figure 6 for the recombinant mutant β1 Val → Met. Although CO combination with deoxyHb is autocatalytic, for purposes of comparison the time courses of these reactions were fitted to single exponentals and average second-order rate constants calculated. The results are summarized in Table IV, where the effects of both IHP and DPG are given. Within error, the CO-binding kinetics of these mutants in the absence of organic phosphate are all identical to normal Hb. In the presence of organic phosphate the CO-binding kinetic properties of the β1 + Met mutant are notably perturbed relative to normal Hb, while the other two mutants are the same as normal Hb.

Table III: Rate Constants for CO Recombination to Normal Hb and β1 Mutants Measured by Flash Photolysis in the Absence of Organic Phosphates[a]

hemoglobin	rate constants/M^{-1} s^{-1}[b] fast	slow
HbA	5.6×10^6	1.7×10^5
β1 Val → Ala	5.9×10^6	1.7×10^5
β1 Val → Met	5.2×10^6	1.4×10^5
β1 + Met	5.4×10^6	1.7×10^5

[a] Conditions: bis-Tris and 100 mM chloride, pH 7, and 20 °C. [b] The precision of the rate constants is approximately 5% (see Experimental Procedures).

Table IV: Rate Constants for CO Combination to Normal Hb and β1 Mutants Obtained from Stopped-Flow Measurements[a]

mutation	conditions	rate const($\times 10^5$)/M^{-1} s^{-1}[b] mutant	HbA
β1 Val → Met	pH 6	1.7	1.5
	pH 6 + 0.1 mM DPG	1.2	1.3
	pH 7	1.8	1.7
	pH 7 + 0.1 mM DPG	1.4	1.4
	pH 7	1.7	1.8
	pH 7 + 0.1 mM IHP	0.94	0.88
	pH 8	2.8	3.2
	pH 8 + 0.1 mM DPG	2.4	2.9
β1 + Met	pH 7	1.9	1.7
	pH 7 + 0.1 mM DPG	1.9	1.5
	pH 7	1.9	1.8
	pH 7 + 0.1 mM IHP	1.3	0.9
β1 Val → Ala	pH 7	1.9	1.9
	pH 7 + 0.1 mM DPG	1.3	1.2
	pH 7	1.9	1.9
	pH 7 + 0.1 mM IHP	0.95	0.95

[a] Conditions: bis-Tris and 100 mM chloride and 20 °C. [b] The precision of the rate constants is approximately 5% (see Experimental Procedures).

Table V: Rates of O_2 Dissociation from Normal Hb and β1 Mutants[a]

hemoglobin	rate const/s^{-1}[b] pH 7	pH 7 + 0.1 mM DPG
HbA	26	52
β1 + Met	22	ND[c]
β1 Val → Met	28	55
β1 Val → Ala	31	ND

[a] Conditions: bis-Tris and 100 mM chloride and 20 °C. [b] The precision of the rate constants is approximately 5% (see Experimental Procedures). [c] Not determined.

Kinetics of Oxygen Dissociation. Rates of O_2 dissociation from the fully oxygenated mutant and normal Hb's in the absence of organic phosphates were measured, as well as the dissociation rates in the presence of DPG for the β1 Val → Met mutant and normal Hb (Table V). The observed rates, which reflect average properties of liganded tetramer and dimer species, are similar to that observed for normal Hb. Again the greatest similarity between normal Hb and the mutants is seen for the β1 Val → Met mutant. The effect of 1 mM DPG on the O_2 dissociation rates of the β1 Val → Met mutant was found to be identical to normal Hb as well.

Bohr Effect of the β1 Val → Met Mutant. One of the most characteristic functional properties of normal Hb is the pH dependence of its O_2 affinity, i.e., the Bohr effect [see Ho and Russu (1987) and Riggs (1988) for recent reviews]. Before concluding that β1 Val → Met was a suitable model for normal Hb it was therefore important to evaluate its Bohr effect. These measurements, which were carried out by traditional tonometry at a single Hb concentration, are less precise than isotherms measured with the Imai cell and lack correction for the presence of dimers. On the other hand, tonometry requires far less time and material and is expected to provide a good estimate of the overall Bohr proton linkage. In particular, the similarities in subunit assembly free energies for the β1 Val → Met mutant and normal Hb indicate that studies done in parallel will provide a good approximation to the comparative effects of pH. The data in Figure 7 show that the functional dependence of oxygen affinity with pH is the same for the mutant and normal Hb. The mutant has a slightly lower oxygen affinity over the entire pH range.

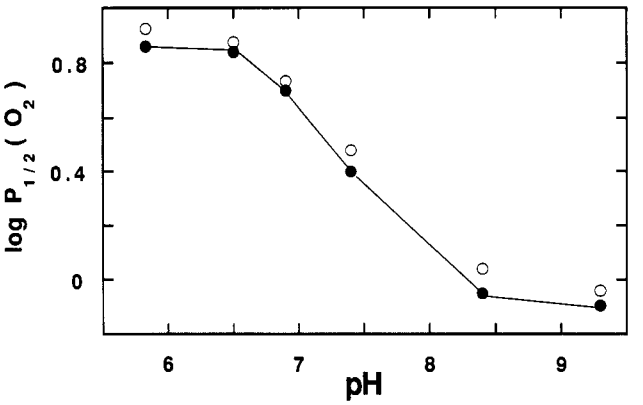

FIGURE 7: Effect of pH on oxygen affinity of HbA (●) and the mutant β1 Val → Met (○). The logarithm of oxygen partial pressure at half-saturation, $P_{1/2}$, is plotted as a function of pH. Measurements were carried out at 20 °C in bis-Tris (or Tris, above pH 7.2) at a constant total chloride concentration of 100 mM and heme concentration of 50 μM.

DISCUSSION

Overall Linkage between Oxygenation and Dimer–Tetramer Assembly. The overall Gibbs energies for oxygenation and subunit assembly refer to the thermodynamic distances depicted in eq 3.

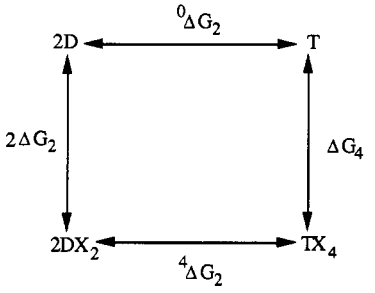

(3)

Here dimers, tetramers, and oxygen are denoted by D, T, and X, respectively. While the overall energetics do not reveal the behavior of the intermediate ligation states, they do provide accurate measures of the overall oxygen affinities of dimers and tetramers and the stabilities of tetramer formation in the fully oxygenated and deoxygenated states. For example, analysis of the p_m data in Figure 1 reveals that the overall oxygen affinities for dimers and tetramers of the mutants are very similar to those of normal Hb. The functional dependencies of p_m on Hb concentration for the mutants are also seen to parallel normal Hb, demonstrating similar dimer–tetramer assembly free energies in both oxy and deoxy states. Quantitative measures of these properties are summarized in Table I. The dimer–tetramer assembly free energies of the fully oxygenated mutants indicate a slight destabilization of the tetramers relative to normal Hb. Experimental studies on these Hb's, such as oxygenation, would therefore reflect an

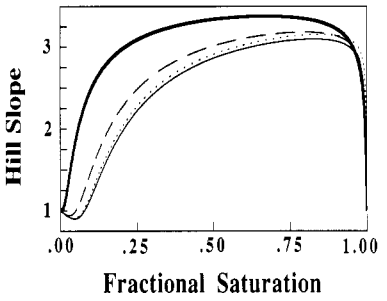

FIGURE 8: Slope of the Hill plot versus fractional saturation for normal HbA_0 [from Chu et al. (1984), thick solid curve] and the recombinant mutant human hemoglobins β1 Val → Ala (dotted curve), β1 Val → Met (dashed curve), and β1 + Met (thin solid curve). Curves were calculated from tetrameric Adair equilibrium constants, K_{4i}, obtained from global regression analysis of multiple isotherms according to eqs 2 and A1. The maximum Hill slopes are 3.38, 3.15, 3.18, and 3.10, respectively. Conditions as in Figure 1.

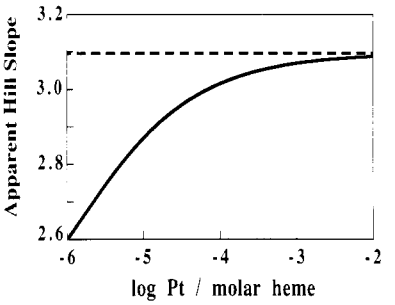

FIGURE 9: Apparent maximum Hill slope as a function of the logarithm of the Hb concentration. The true maximum Hill slope (dashed line) corresponds to the pure tetrameric properties of the β1 + Met mutant. The apparent Hill slope corresponds to the observed maximum Hill slope when correction for the presence of dimers is not made. Conditions as in Figure 1.

increased contribution from the dimers by approximately 2-fold. In contrast, a small increase in tetramer stability was seen for the deoxygenated form of the β1 Val → Met mutant.

The overall energetics described by eq 3 also provide a measure of the sum of all regulatory free energy used to modulate the intrinsic O_2-binding free energy of the protomers [see Ackers et al. (1992) for recent review], either as $\alpha\beta$ dimers or equivalently as the average of the pure α and β chains (Valdes & Ackers, 1977; 1978; Mills et al., 1979)). This quantity, the overall cooperative free energy ΔG_c, is a thermodynamic property of the entire tetrameric molecule and is measured as the difference between oxy and deoxy dimer–tetramer assembly free energies or the difference between overall oxygen-binding free energies of tetramers and dimers (Ackers & Smith, 1987).

$$\Delta G_c = {}^4\Delta G_2 - {}^0\Delta G_2 = \Delta G_4 - 2\Delta G_2 \qquad (4)$$

The cooperative free energies for normal Hb (Chu et al., 1984) and the recombinant mutant Hb's β1 Val → Ala, β1 Val → Met, and β1 + Met are 6.3 ± 0.14, 6.45 ± 0.10, 7.50 ± 0.11, and 7.09 ± 0.10 kcal, respectively. Thus the cooperative free energies of the β1 mutants are not significantly perturbed. Since β1 Val is located externally on the protein, these findings are consistent with extensive structure–function studies of the cooperative free energies of 59 mutant and chemically modified human Hb's, which demonstrated that large perturbations in the cooperative free energy were mainly due to structural modifications within the $\alpha^1\beta^2$ interface (Pettigrew et al., 1982; Turner, 1989; Turner et al., 1992).

Cooperativity within Dimers and Tetramers. Figure 3 summarizes the stepwise oxygenation energetics of dimers and tetramers for the recombinant Hb's. Stepwise oxygen binding by the dimers all show, within error, noncooperative behavior in agreement with the binding properties of normal Hb dimers [Mills et al. (1976) and Chu et al. (1984); see also Fiugre 3].

Cooperativity within the β1 mutant tetramers is portrayed in Figure 8 as the slope of their Hill plots [cf. Edsall and Gutfreund (1983)] versus fractional saturation. All three mutants exhibit a remarkable degree of cooperativity, with the lowest maximum Hill slope being 3.10. Moreover, the asymmetric dependence of Hill slope on fractional saturation (higher cooperativity at higher fractional saturation) is maintained. These findings argue strongly that the side chain of β1 valine does not play a critical role in cooperative oxygen binding by hemoglobin. The high cooperativity manifested by the β1 + Met mutant argues against a significant contribution from the amino terminal portion of the residue as well.

Practical Importance for Including Dimer–Tetramer Assembly Equilibria during Oxygenation Studies. The experimental strategy we have employed for determining oxygen-binding equilibria involves global analysis of oxygenation isotherms measured over a range of Hb concentration. Although this procedure is much more laborious than traditional procedures (which involve evaluation of a single oxygenation isotherm) there are clear benefits, especially for studies aimed at understanding the thermodynamic mechanism. First, most of the instrumentation currently available for measuring oxygenation isotherms are best suited for precise measurements in the 1–100 μM heme range of Hb concentration. Since the oxygenated forms of most human Hb tetramers are substantially dissociated into dimers at these concentrations, the shapes of the measured isotherms reflect properties of dimers and tetramers. Thus assignment of measured quantities (such as the maximum Hill slopes, p_{50}'s, or apparent equilibrium constants) to an assumed pure tetrameric species can be misleading. These complications will be most problematic for mutations at the critical $\alpha^1\beta^2$ interface which tend to destabilize the tetramer the largest amount (Turner et al., 1992).

Mutagenesis at the β1 position is found in the present study to be relatively innocuous with regard to the dimer–tetramer equilibrium. Nevertheless, comparison of the true maximum Hill slope of the β1 + Met mutant to the apparent maximum Hill slope obtained from isotherms without correction for the presence of dimers shows a concentration-dependent potential for misinterpretation (Figure 9). Whether an apparent Hill slope provides sufficient information to the researcher depends on the Hb concentration as well as the questions being investigated. More extensive analyses of the bias error caused from not correcting for the presence of dimers have been given previously (Johnson & Ackers, 1977; Johnson & Lassiter, 1990).

Dimer–Tetramer Assembly at Intermediate Oxygenation States. Another benefit of explicit consideration of the linkage between oxygenation and subunit assembly comes from the additional information gained by correlating tetrameric heme–heme interaction energies with changes in dimer–tetramer assembly free energy. The assembly free energies provide a sensitive measure of cooperativity-linked structure changes at the $\alpha^1\beta^2$ interface. The fundamental role that the $\alpha^1\beta^2$ interface plays in cooperativity is born out by structure–function studies (Pettigrew et al., 1982; Turner, 1989, Turner et al., 1992) and X-ray crystallographic analysis (Baldwin & Chothia, 1979; Shaanan, 1983).

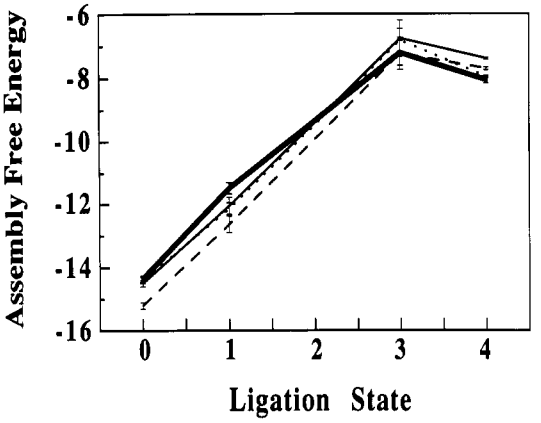

FIGURE 10: Dimer–tetramer assembly free energy versus tetramer ligation state for normal Hb [from Chu et al. (1984), thick solid curve] and the recombinant human hemoglobins β1 Val → Ala (dotted curve), β1 Val → Met (dashed curve), and β1 + Met (thin solid curve). Error bars represent the largest deviation of the upper and lower 67% confidence limits and are plotted symmetric about each point. Conditions as in Figure 1.

Figure 10 displays the relationship between ligation state and alterations in assembly free energy. The general pattern seen for all these Hb's is a progressive destabilization of the dimer–dimer interaction energies upon oxygenation at low saturations. Upon binding the last oxygen, however, the tetramer is stabilized by approximately 0.5 kcal in each case. It follows that the O_2 affinity of the last binding step of the tetramer is enhanced relative to that of the dimer. This effect, called quaternary enhancement (Mills & Ackers, 1979b), has been found for O_2 binding to normal Hb over a variety of conditions (Mills & Ackers, 1979a; Chu et al., 1984). It has also been reported from partially ligated intermediate studies (Speros et al., 1991) and oxygenation studies with cobaltous hemoglobin (Doyle et al., 1991). The similar pattern of cooperative switching at the $\alpha^1\beta^2$ interface found with the β1 mutants and normal Hb suggests a common cooperative mechanism.

CO Binding Kinetics and Heterotropic Regulation by Organic Phosphates and Protons. In the absence of organic phosphates the CO-binding kinetics of the β1 mutant Hb's mimic normal Hb quite closely (Tables III and IV). These findings, measured by stopped-flow and flash photolysis methods, demonstrate normal CO-binding dynamic behavior of the deoxygenated β1 mutant dimers and tetramers. The kinetics probe CO binding at the heme sites per se, but more importantly they are sensitive to the dynamics of all linked tertiary and quaternary conformational changes. The rates of O_2 dissociation from these hemoglobins are also found to be quite normal (Table V).

In addition to the cooperative interactions between heme-site ligands themselves, regulation of oxygen affinity in Hb also involves linkage to secondary ligands such as protons and organic phosphates. The question then arises whether β1 Val plays a significant role in these allosteric processes and, if so, whether the β1 mutations studied here alter the allosteric behavior. Since organic phosphates bind at the β1 amino termini (Arnone, 1972; Arnone & Perutz, 1974), investigation of the allosteric effects of organic phosphates on the β1 mutants is particularly germane.

Comparison of the organic phosphate-induced change in CO-binding kinetics of the β1 mutants to normal Hb shows (Table IV, Figure 6) the β1 Val → Met and β1 Val → Ala mutants to be normal, whereas the allosteric effect of DPG is absent in the case of the β1 + Met mutant and diminished with IHP. This perturbed allosteric behavior of the β1 + Met mutant is consistent with a reduced organic phosphate-binding affinity of the deoxy structure. Allosteric effects of organic phosphates can also be probed by considering the effect of IHP on the dimer–tetramer equilibrium. Here the equilibrium between dimers and tetramers will shift according to the relative IHP-binding affinities and stoichiometries of dimers versus tetramers, as well as ionic strength effects (Hensley et al., 1975; White, 1976; Turner, 1984). As such, simple correlations to tetrameric IHP-binding affinities alone are difficult, and we therefore limit our interpretations to a consistency test of IHP effects on the β1 mutants and normal Hb. The mutant which shows the greatest similarity in its dimer–tetramer equilibrium as a function of IHP is the β1 Val → Met mutant (Figure 5). In contrast, at millimolar concentrations of IHP the β1 Val → Ala mutant shows an extra 0.8 kcal of destabilization, while the β1 + Met mutant shows an extra 0.6 kcal of IHP-related stabilization when compared to normal Hb.

The molecular origin of the pattern of organic phosphate effects seen with the β1 mutants is likely to come from localized structural perturbations at the β1 amino termini due to the mutations. Since the isopropyl side chain of β1 Val is nonpolar, uncharged, and located on the external portion of the tetramer, it likely plays a relatively minor allosteric role, while the more reactive terminal amino group is likely to be of critical importance. If so, one would expect that replacement of β1 Val by nonpolar, moderately sized residues (such as alanine) would preserve the allosteric response. Crystallographic structure analysis on the three β1 mutants (Kavanaugh et al., 1992) shows the organic phosphate-binding site on the β1 + Met mutant to be perturbed by the greatest amount, as expected from the presence of an extra amino acid residue at the amino terminus. The β1 Val → Ala mutant was found to exhibit some structural distortion in this region and a decrease in the phosphate-associated electron density. In contrast, the X-ray crystallographic work found the β1 Val → Met mutant to be the least perturbed in this region.

In view of typical pK values for amino termini (8.0), and the ligand-linked structure changes at the β1 position (Fermi et al., 1984: Shaanan, 1983), it seems reasonable that the amino terminus of β1 Val would contribute to the Bohr effect. This observation has been pointed out previously (Perutz et al., 1980), and extensive computational investigations of the Bohr effect indicate a substantial Bohr contribution from β1 Val (Garcia-Moreno, B. and Ackers, G. K., unpublished observations). Figure 7 shows the pH dependence of the logarithm of the half-saturation O_2 partial pressures for normal Hb and the β1 Val → Met mutant. The slopes of these functions at a given pH approximate the number of protons linked to the overall oxygenation of the two Hb's and are found, within error, to be identical (at pH 7.4 for example, 0.52 ± 0.07 protons released per O_2). Thus, the β1 Val → Met mutation is functionally silent with regard to the overall Bohr effect. This may be due to either the similarity in chemical environments of the amino group on the methionine compared to the native valine residue or the Bohr contribution of the normal β1 valine amino terminus itself may be small.

Another physiological effector of Hb function which is known to exert approximately half of its effect through the amino group of β1 Val is carbon dioxide [see Doyle et al. (1987) and references therein]. The present study has shown that the β1 Val → Met mutant has a normal allosteric response to organic phosphates and pH, arguing that the amino terminus is the primary allosteric group of β1 Val and the side chain

is of secondary importance (providing no large changes in size or polarity are made). If this concept is correct, then a normal CO_2 allosteric response is also predicted for the β1 Val → Met mutant.

Choosing a Reference Structure. The present examination of equilibrium and kinetic functional properties of the three recombinant mutant Hb's (β1 Val → Ala, β1 Val → Met, and β1 + Met) provides an unprecedented degree of detail in evaluating the ability of recombinant strategies to produce multimeric proteins with normal allosteric behavior. The normal subunit assembly and cooperative oxygenation properties of the mutants clearly demonstrate the functional integrity of the recombinant syntheses, a conclusion amply confirmed by the homogeneity and autocatalytic nature of their CO-binding kinetics. The present results also demonstrate that substitutions can be made at the β1 amino terminus without greatly disrupting the subtle allosteric properties of Hb. On the other hand, none of these recombinant mutants is identical to HbA. The detectable deviations of the mutant Hb's from normalcy are (1) slightly lowered tetramer oxygen affinities, (2) small changes in dimer–tetramer equilibria, and (3) a perturbed allosteric response to organic phosphates by the β1 + Met mutant. The latter effect is presumably due to the bulkiness of adding an additional residue to the amino terminus.

The objective of the present study has been to determine whether certain mutant recombinant human Hb's produced directly in *E. coli.* (Hernan et al., 1992) have normal homotropic and heterotropic regulatory properties. Such a mutant would then serve as a surrogate system for the recombinant production of further mutants for structure–function studies. The present results indicate that any of the three β1 mutants studied could serve this function quite well, although we note that none is identical in all respects to normal HbA_0. We conclude that the β1 Val → Met mutant is particularly attractive for structure–function studies and will serve as our reference system for the following reasons: (1) it binds oxygen with very high cooperativity (maximum Hill slope of 3.18) and displays a slightly higher cooperativity than the other two mutants at low fractional saturations (Figure 8); (2) its allosteric response to organic phosphates was found to be identical to normal Hb; (3) it shows an overall linkage to protons equal to that of normal Hb; and (4) only minor localized changes were detectable between its crystallographic structure and that of normal Hb (Kavanaugh et al., 1992).

APPENDIX

The fractional saturation, $\bar{Y}$, of the chemical species in eq 1 is a function of seven independent equilibrium constants as well as the protein concentration, P_t (heme units), and the ligand activity, [X].

$$\bar{Y} = \frac{Z_2 + Z'_4[\sqrt{(Z_2)^2 + 4\,{}^0K_2Z_4P_t} - Z_2]/(4Z_4)}{Z_2 + \sqrt{(Z_2)^2 + 4\,{}^0K_2Z_4P_t}} \quad \text{(A1)}$$

Here the binding polynomials for dimers (Z_2) and tetramers (Z_4) are

$$Z_2 = 1 + K_{21}[X] + K_{22}[X]^2$$

$$Z'_2 = K_{21}[X] + 2K_{22}[X]^2$$

$$Z_4 = 1 + K_{41}[X] + K_{42}[X]^2 + K_{43}[X]^3 + K_{44}[X]^4$$

$$Z'_4 = K_{41}[X] + 2K_{42}[X]^2 + 3K_{43}[X]^3 + 4K_{44}[X]^4$$

where the prime superscripts indicate first derivatives with respect to the logarithm of [X]. The Adair equilibrium constants, K_{ij}, in the binding polynomials refer to equilibria between the deoxygenated dimers ($i = 2$) or tetramers ($i = 4$) and the state with j oxygens bound. The stepwise free energies reported in Figure 3, on the other hand, refer to intrinsic stepwise equilibria for binding the jth oxygen to a dimer or tetramer with $j - 1$ oxygens already bound. These intrinsic stepwise equilibrium constants k'_{ij} are calculated from the Adair constants and a statistical degeneracy term as

$$k'_{ij} = \left(\frac{j}{i-j+1}\right)\left(\frac{K_{ij}}{K_{i(j-1)}}\right) \quad \text{(A2)}$$

The free energies for the overall binding of four oxygens to tetramers or two oxygens to dimers are denoted by ΔG_4 and ΔG_2, respectively (eq 3). Dimer–tetramer assembly equilibrium constants are defined for the jth ligation state of the tetramer as

$${}^jK_2 = \frac{[TX_j]}{[DX_k]\,[DX_l]} \quad \text{(A3)}$$

where $k + l = j$ and $k, l = 0, 1, 2$. Likewise, the corresponding subunit assembly free energies are denoted by ${}^j\Delta G_2$.

The median partial pressure, p_m, of an isotherm is a measure of the chemical work for complete saturation of the macromolecule and can be found as the partial pressure where the areas above and below the isotherm are equal [cf. Wyman and Gill (1990)].

$$\int_{[X]=0}^{[X]=[P_m]} \bar{Y}\, d \ln [X] = \int_{[X]=[p_m]}^{[X]=\infty} (1 - \bar{Y})\, d \ln [X] \quad \text{(A4)}$$

Median analysis for ligand-linked dimerizing systems is especially useful for determining the overall subunit assembly and oxygenation energies of the system. The median varies with protein concentration, P_t, according to three overall equilibrium constants: K_{44}, ${}^0K_2$, and ${}^4K_2$ (Johnson et al., 1976).

$$p_m = \sqrt[4]{\left[K_{44}^{-1}\frac{1 - {}^4f_2}{1 - {}^0f_2}\exp({}^0f_2 - {}^4f_2)\right]} \quad \text{(A5)}$$

where

$${}^0f_2 = \frac{\sqrt{1 + 4[P_t]\,{}^0K_2} - 1}{2[P_t]\,{}^0K_2} \quad \text{(A6)}$$

$${}^4f_2 = \frac{\sqrt{1 + 4[P_t]\,{}^4K_2} - 1}{2[P_t]\,{}^4K_2} \quad \text{(A7)}$$

The fraction of dimer species for the unliganded and fully liganded systems are designated by ${}^0f_2$ and ${}^4f_2$, respectively.

REFERENCES

Ackers, G. K. (1970) *Adv. Prot. Chem. 24*, 343–446.
Ackers, G. K., & Halvorson, H. R. (1974) *Proc. Natl. Acad. Sci. U.S.A. 91*, 4312–4316.
Ackers, G. K., & Smith, F. R. (1987) *Annu. Rev. Biophys. Biophys. Chem. 16*, 583–609.
Ackers, G. K., Johnson, M. L., Mills, F. C., Halvorson, H. R., & Shapiro, S. (1975) *Biochemistry 14*, 5128–5134.
Ackers, G. K., Doyle, M. L., Myers, D., & Daugherty, M. A. (1992) *Science 255*, 54–63.
Arnone, A. (1972) *Nature (London) 237*, 146–149.
Arnone, A., & Perutz, M. F. (1974) *Nature (London) 249*, 34–36.
Allen, D. W., Guthe, K. F., & Wyman, J. (1950) *J. Biol. Chem. 187*, 393–410.
Baldwin, J., & Chothia, C. (1979) *J. Mol. Biol. 129*, 175–220.
Bevington, P. R. (1969) *Data Reduction and Error Analysis for the Physical Sciences*, McGraw-Hill, New York.
Chu, A. H., & Ackers, G. K. (1981) *J. Biol. Chem. 256*, 1199–1205.
Chu, A. H., Turner, B. W., & Ackers, G. K. (1984) *Biochemistry 23*, 604–617.
Doyle, M. L., & Ackers, G. K. (1992) *Biophys. Chem. 42*, 271–281.
Doyle, M. L., Di Cera, E., Robert, C. H., & Gill, S. J. (1987) *J. Mol. Biol. 196*, 927–934.
Doyle, M. L., Di Cera, E., & Gill, S. J. (1988) *Biochemistry 27*, 820–824.
Doyle, M. L., Speros, P. C., LiCata, V. J., Gingrich, D., Hoffman, B. M., & Ackers, G. K. (1991) *Biochemistry 30*, 7263–7271.
Draper, N. R., & Smith, H. (1981) *Applied Regression Analysis*, 2nd ed., J. Wiley & Sons, Inc., New York.
Edsall, J. T., & Gutfreund, H. (1983) *Biothermodynamics: The Study of Biochemical Processes at Equilibrium*, J. Wiley & Sons, Inc., New York.
Fermi, G., Perutz, M. F., Shaanan, B., & Fourme, R. (1984) *J. Mol. Biol. 175*, 159–174.
Geraci, G., Parkhurst, L. J., & Gibson, Q. H. (1969) *J. Biol. Chem. 244*, 4668.
Gibson, Q. H. (1959) *Biochem. J. 71*, 293.
Gibson, Q. H., & Milnes, L. (1964) *Biochem. J. 91*, 161.
Haire, R. N., & Hedlund, B. E. (1977) *Proc. Natl. Acad. Sci. U.S.A. 74*, 4135–4138.
Hayashi, A., Suzuki, T., & Shin, M. (1973) *Biochim. Biophys. Acta 310*, 310–316.
Hensley, P., Moffat, K., & Edelstein, S. J. (1975) *J. Biol. Chem. 250*, 9391–9396.
Hernan, R. A., Hui, H. L., Andracki, M. E., Noble, R. W., Sligar, S. G., Walder, J. A., & Walder, R. Y. (1992) *Biochemistry* first paper of three in this issue.
Ho, C., & Russu, I. M. (1987) *Biochemistry 26*, 6299–6305.
Hoffman, S. J., Looker, D. L., Roehrich, J. M., Cozart, P. E., Durfee, S. L., Tedesco, J. L., & Stetler, G. L. (1990) *Proc. Natl. Acad. Sci. U.S.A. 87*, 8521–8525.
Imai, K. (1982) *Allosteric Effects in Haemoglobin*, Cambridge University Press, Cambridge, London.
Imaizumi, K., Imai, K. & Tyuma, I. (1979) *J. Biochem. 86*, 1829–1840.
Ip, S. H. C., Johnson, M. L., & Ackers, G. K. (1976) *Biochemistry 15*, 654–659.
Johnson, M. L., & Ackers, G. K. (1977) *Biophys. Chem. 7*, 77.
Johnson, M. L., & Frasier, S. G. (1985) *Methods Enzymol. 117*, 301–342.
Johnson, M. L., & Lassiter, A. E. (1990) *Biophys. Chem. 37*, 231–238.
Johnson, M. L., Halvorson, H. R., & Ackers, G. K. (1976) *Biochemistry 15*, 5363–5371.
Kavanaugh, J. S., Rodgers, P. H., & Arnone, A. (1992) *Biochemistry* (third paper of three in this issue).
Matheson, I. B. C. (1987) *Anal. Instrum. 6*, 345–351.
Mills, F. C., & Ackers, G. K. (1979a) *J. Biol. Chem. 254*, 2881–2887.
Mills, F. C., & Ackers, G. K. (1979b) *Proc. Natl. Acad. Sci. U.S.A. 76*, 273–277.
Mills, F. C., Johnson, M. L., & Ackers, G. K. (1976) *Biochemistry 15*, 5350–5362.
Mills, F. C., Ackers, G. K., Gaud, H. T., & Gill, S. J. (1979) *J. Biol. Chem. 254*, 2875–2880.
Nagai, K., & Thøgersen, H. C. (1984) *Nature 309*, 810–812.
Nagai, K., Perutz, M. F., & Poyart, C. (1985) *Proc. Natl. Acad. Sci. U.S.A. 82*, 7252–7255.
Nagel, R. L., Wittenberg, J. B., & Ranney, H. M. (1965) *Biochim. Biophys. Acta 100*, 286–289.
Pettigrew, D. W., Romeo, P. H., Tsapis, A., Thillet, J., Smith, M. L., Turner, B. W., & Ackers, G. K. (1982) *Proc. Natl. Acad. Sci. U.S.A. 79*, 1849–1853.
Perutz, M. F., Kilmartin, J. V., Nishikura, K., Fogg, J. H., Butler, P. J. G., & Rollema, H. S. (1980) *J. Mol. Biol. 138*, 649–670.
Riggs, A. F. (1981) *Methods Enzymol. 76*, 5–29.
Riggs, A. F. (1988) *Annu. Rev. Physiol. 50*, 181–204.
Shaanan, B. (1983) *J. Mol. Biol. 171*, 31–59.
Speros, P. C., LiCata, V. J., Yonetani, T., & Ackers, G. K. (1991) *Biochemistry 30*, 7254–7262.
Steimeier, R. C., & Parkhurst, L. J. (1975) *Biochemistry 14*, 1564–1572.
Turner, B. W. (1984) Ph.D. dissertation, The Johns Hopkins University.
Turner, G. J. (1989) Ph.D. dissertation, The Johns Hopkins University.
Turner, G. J., Galacteros, F., Doyle, M. L., Turner, B. W., Pettigrew, D. W., Smith, F. R., Hedlund, B., Moo-Penn, W., Rucknagel, D. L., & Ackers, G. K. (1992) *Proteins* (in press).
Valdes, R., & Ackers, G. K. (1977) *J. Biol. Chem. 252*, 74–81.
Valdes, R., & Ackers, G. K. (1978) *Proc. Natl. Acad. Sci. U.S.A. 75*, 311–314.
Wagenbach, M., O'Rourke, K., Vitez, L., Wieczorek, A., Hoffman, S., Durfee, S., Tedesco, J., & Stetler, G. (1991) *Biotechnology 9*, 57–61.
White, S. L. (1976) *J. Biol. Chem. 251*, 4763–4769.
Wyman, J., & Gill, S. J. (1990) *Binding and Linkage: Functional Chemistry of Biological Macromolecules*, University Science Books, Mill Valley, CA.

Registry No. HbA, 9034-51-9; IHP, 83-86-3; Val, 72-18-4; Ala, 56-41-7; Met, 63-68-3; CO, 630-08-0; O_2, 7782-44-7; H^+, 12408-02-5.